Assessing the ecological risk of pesticides should not ignore the impact of their transformation byproducts - the case of Chlorantraniliprole

Meng Wu[a], Guilong Li[a], Pengfa Li[a], Nan Jiang[a], Shiping Wei[b], Evangelos Petropoulos[c], Zhongpei Li[a,*]

[a]*State Key Laboratory of Soil and Sustainable Agriculture, Institute of Soil Science, Chinese Academy of Sciences, Nanjing 210008, PR China*

[b]*Jiangsu Engineering and Technology Center for Modern Horticulture, Jiangsu Polytechnic College of Agriculture and Forestry, Zhenjiang, Jiangsu 212400, PR China*

[c]*School of Engineering, Newcastle University, Newcastle upon Tyne NE1 7RU, UK*

Corresponding Author

Zhongpei Li —Beijing East Road No. 71, Nanjing 210008, PR China. E-mail: zhpli@issas.ac.cn

1. Introduction

Degradation of pesticides involves the transformation of their molecules, via alteration and/or break down, to a series of molecular byproducts (Roberts and Hutson, 1999). In most cases, biota in agricultural ecosystems is exposed to a mixture of pesticides and their transformation byproducts (Felicio et al., 2018; Girones et al., 2020). Such transformation byproducts may contain toxic nucleus and active components from the parent pesticides that can affect the quality of the ecosystem or of the overall environment (Sinclair and Boxall, 2003). The physicochemical and toxicological properties of these transformation products may differ from those of the parent pesticides, and subsequently they often affect random non-target organisms. In a previous study, the toxicity of 60 active compounds was compared with that of their transformation byproducts; the result showed that 30% of the byproducts were more toxic, and 4.2% of the byproducts exhibited more than tenfold higher toxicity from the original substance (Sinclair and Boxall, 2003). Additionally, there are transformation byproducts, from a wide range of pesticides, which are more persistent against degradation than their parent compounds (Boxall et al., 2004). In recent years, pesticide transformation byproducts attracts more and more attention and have been classified into the category of "emerging contaminants" (Pietrzak et al., 2020). Therefore, it is imperative to clarify the dissipation process of pesticides and identity the properties of their transformation byproducts. However, the information related to such transformation byproducts is limited, especially for numerous, recently-developed

pesticides; this may inevitably lead to underestimation of the ecological risk from these pesticides.

As such, Chlorantraniliprole (CAP, Fig. 1) is a novel anthranilic diamide insecticide developed by DuPont Crop Protection (Lahm *et al*., 2005). This insecticide has been registered with a name "Rynaxypyr" and is widely used in the paddy fields of China (Zhang et al., 2012). The insecticidal activity and the operational pathway of CAP is well studied (Cordova et al., 2006; Teixeira et al., 2009). CAP shows low toxicity to many non-target organisms such as birds and mammals (Lahm et al., 2007). Soil microbial organisms are sensitive to external disturbance/factors; thus, they could serve as a good indicator of the status of soil health when this is subjected to changes (Pimentel et al. 2005). Previous studies have showed that CAP could significantly affect both the microbial activity and community composition in soil (Wu et al., 2017, 2018), especially under high application doses (i.e. 10 mg kg^{-1} a.i./dw). However, whether the CAP transformation byproducts could significantly affect the soil microbe is a question that remains unanswered. Soil is a sink of pesticides; thus, it is expected that pesticides and their transformation byproducts could significantly affect the soil microbiome as a response towards an ecological risk. Although research groups have identified the chemical structures and the potential impact for many of the CAP hydrolysis (Sharm et al., 2014) and photolysis products (Gaddamidi et al., 2011; Redman et al., 2020), the transformation byproducts of this pesticide in soil have been limited unexplored, likely due to their low concentrations and the difficulty of their extraction from the soil medium. To our knowledge, previous literatures only reported one CAP degradation

byproduct in soil environment so far (Redman et al., 2019), however, whether there are more transformation byproducts and how they affect the soil ecosystem still remains unclear.

In this study, to further understand the impact of CAP degradation byproducts on soil we carried out the following: 1) extraction of the main CAP transformation byproducts from soil and identification of their chemical structures; 2) study the dissipation process of CAP and its transformation byproducts; 3) investigation of the effect of CAP and its transformation byproducts on the soil microbial community structure. Through this study, we seek to evaluate the ecological risk of the CAP transformation byproducts and to further re-assess the safety of CAP and its life cycle in soil ecosystems.

2. Materials and methods

2.1. Chemicals and Soil samples

The insecticide CAP (98% purity) was purchased from J&K Scientific, China. A silty-loam paddy soil developed from Jurassic purple shale and sandstone was collected from Beibei District, Chongqing City (29°50´ N, 106°25´ E) - in subtropical China. Five replicate treatments were prepared using the topsoils (0–20 cm) of the original paddy field and mixed to form a uniform soil sample. The soil sample was then air-dried and sieved (< 2 mm) prior to further experimentation. The basic physicochemical parameters have been reported in our previously published research (Wu et al, 2018). Briefly, the physicochemical properties of the soil are as follows: sand (26.9%), silt (54.0%), clay (19.1%), pH (7.46), soil organic carbon (15.1 g kg^{-1}), total nitrogen (1.33 g kg^{-1}), total phosphorus (0.63 g kg^{-1}), total potassium (25.0 g kg^{-1}).

84 *2.2. Extraction of potential CAP transformation byproducts in soil*

85 We have previously carried out CAP degradation experiments under two application
86 doses (1 mg/kg and 10 mg/kg), see (Wu et al., 2018). During the degradation trial, we
87 detected three main potential transformation byproducts based on the HPLC
88 spectrograms. To obtain the three compounds, we applied CAP at a higher than
89 previously trialed dose (100 mg/kg in 5 kg soil). The soils were incubated in the dark
90 for 30 days at 25 °C; the soils were maintained with 50% maximum soil waterholding
91 capacity. A well-known residue procedure named "Quick, easy, cheap, effective,
92 rugged, and safe" method (QuEChERS) (Anastassiades et al., 2003) was then applied
93 for the extraction and the cleanup of both CAP residues and the potential transformation
94 byproducts. Briefly, the residues from the soils were extracted twice using acetonitrile
95 (solid-to-liquid ratio is one to four) in batches. The samples were centrifuged at 4000g
96 for 10 min. The combined CAP extracts were concentrated by rotary evaporation to
97 about 50 mL and transferred to a centrifuge tube containing 4.0 g anhydrous MgSO4,
98 0.8 g primary secondary amine (PSA, 40–60 μm) sorbent and 0.8 g C18 bondesil (40–
99 60 μm). After shaking vigorously for 1 min, the tube was centrifuged at 4000g for 2
100 min. The supernatant was rotary evaporated to remove the organic solvents contained,
101 to obtain the crude products (about 0.4 g).

102 One part of the crude products (1 mg) was used to detect the potential byproducts, to
103 do so it was re-dissolved in 100 mL methanol and filtered through a 0.22 μm filter
104 (Millipore, USA) prior to high performance liquid chromatography (HPLC) analysis.
105 A Shimadzu analytical HPLC was equipped with a SPD-M20A detector and a

reversed–phase C18 column (Agilent Zorbax Eclipse XDB-C18, 4.6 mm ×150 mm, 5 μm) which was kept at 40 ℃. The CAP detection wavelength used was 260 nm. The injection volume was 20 μL and the flow rate of mobile phase (mobile phase A: water, mobile phase B: acetonitrile) was 0.6 mL min^{-1}. The total running time was 22.0 min and the linear gradient of the mobile phase (v/v, %) was set as 60% B at 0 min, 100% B at 10 min, 100% B at 15 min, 60% B at 15.1 min, and 60% B at 22 min. The retention time (RT) of CAP in the HPLC spectrogram (Fig. S1) was 5.396 min. The three compounds Z1 (4.068 min), Z2 (8.943 min), and Z3 (11.957 min) detected in the HPLC spectrogram (Fig. S1) were not present in the blank soil samples (without CAP applied). Thus, Z1, Z2, and Z3 were considered as potential CAP transformation byproducts. The solution was then let standing overnight and was tested again the next day using the same HPLC analysis. The compound Z3 disappeared from the HPLC spectrogram indicating that Z3 was very unstable and difficult to be extracted. Our next goal was to obtain pure Z1 and Z2 compounds.

The remaining crude product was used for the separation of Z1 and Z2 using a preparative chromatograph (Shimadzu LC-20A Prep HPLC) equipped with a Phenomenex Luna C18 column (50 mm×300 mm, 10 μm) operating at room temperature. The detection wavelength was 254 nm. The injection mass was 200 mg and the flow rate of the mobile phase, composed of water-acetonitrile (40:60, v/v), was 80.0 mL min^{-1}. The total running time was 30 min. The separated distillate solution was rotary evaporated to remove organics from the solution, the remained volume was freeze dried to obtain the primary separation products. The above steps were repeated

to obtain pure Z1 and Z2 compounds. The liquid chromatographic purity of Z1 and Z2 were 100% and 95.3% respectively (Fig. S2), at this purity the agents could be used for further chemical structure identification.

2.3. Chemical structure identification

The melting points (mp.) of Z1 and Z2 were determined using a X-4A binocular microscope melting-point apparatus. ^{1}H NMR, ^{13}C NMR and ^{1}H-^{13}C HSQC spectra of Z1 and Z2 were obtained using a Bruker AC-P 400 spectrometer with $CDCl_3$ as solvent. Chemical shifts (δ) are given in parts per million and were measured downfield from internal tetramethylsilane. Chemical shifts (δ) are reported in parts per million using the solvent standard peak as reference. High-resolution mass spectra (HRMS) of Z1 and Z2 were obtained using an Agilent 1200 Series HPLC equipped with an Agilent 6210 TOF mass detector.

2.4. Incubation experiments of CAP and its transformation byproducts in soil

Incubation experiments were conducted with CAP, Z1, and Z2 in 100 mL polyethylene bottles covered with sterile polytetrafluoroethylene membrane which allowed aerobic conditions through air exchange. In each bottle, soil sample (15.0 g) with 50% maximum soil water-holding capacity was added and pre-incubated for a week.15 μL of the CAP, Z1, and Z2 stock solutions (1000 mg L^{-1} in methanol) were then added to give a final concentration of 1 mg kg^{-1} a.i./dw of CAP, Z1, and Z2. Thus, overall four treatments were prepared: Control (CK), CAP (1 mg kg^{-1}), Z1 (1 mg kg^{-1}), and Z2 (1 mg kg^{-1}). Control samples (CK) were prepared by adding 15 μL methanol without CAP, Z1, or Z2. All samples were placed in a fume cabinet for 2 hours to

remove methanol (through evaporation) and then they were thoroughly mixed. The samples with 50% maximum soil waterholding capacity were placed in an incubator at 25 °C and kept in the dark for 78 days. Four replicate bottles from each treatment were randomly removed from the environmental chamber at different incubation time intervals (7, 14, 25, 36, and 78 days). All treatments were collected for residues analysis. The soil samples collected at day 7, 14, 25 and 36 were used to extract soil DNA for bacterial community analysis.

The QuEChERS method mentioned above (Section 2.2) was used again for the extraction and cleanup of the CAP, Z1, and Z2 residues in soil. The residues were quantified by HPLC analysis (mentioned above). The standard solutions (0.1, 0.5, 1.0, 5.0, and 10.0 mg L^{-1}) was used to form calibration curves for CAP, Z1, and Z2. The calibration curves showed relatively good linearity (r^2 = 0.9983~0.9995 for the three compounds). According to the previous research (Wu et al., 2017), the recovery tests of CAP, Z1, Z2 were conducted in three additional levels (0.1, 0.5, and 1mg kg^{-1} a.i./dw). The recoveries of CAP, Z1, and Z2 in the soil were 86.4–92.3%, 83.0–85.1%, and 80.9–87.1%, respectively. An acceptable analytical method is considered when analytes range between 70% to 110% (Schwarz *et al*., 2011), the HPLC method employed here was considered valid and reliable measuring the residues of CAP and its transformation byproducts in soil.

2.5. Soil DNA extraction, MiSeq pyrosequencing and Bioinformatics analysis

Soil total DNA was extracted from 0.50 g of each soil sample using a FastDNA™ SPIN Kit (MP Biomedicals, Santa Ana, USA) following the manufacturer's

instructions. The V4-V5 hypervariable region of bacterial 16S rRNA gene was amplified using primer sets: 515F (5'-GTGCCAGCMGCCGCGGTAA-3') and 907R (5'-CCGTCAATTCMTTTRAGTTT-3'). For each PCR reaction, 50 μL of mixture was prepared and included 2x Premix Taq (25 μL), 10 mM Primer-F (1 μL), 10 mM Primer-F (1 μL), 20 ng/μL g-DNA (3 μL) and nuclease-free water (20 μL). Illumina libraries were constructed using the MiSeq platform using MiSeq v3 Reagent Kit (Illumina Inc., CA, US). Raw data of Illumina sequencing were selected based on the sequence length and quality using Mothur and QIIME software (Caporaso et al., 2010; Schloss et al., 2009). Sequences with less than 200 bp in length and the reads containing any unresolved nucleotides were removed. The assembled reads were processed by de novo chimera detection conducted with UCHIME (Edgar et al., 2011). Next, the unique sequence set was clustered into operational taxonomic units (OTUs) at the threshold of 97% identity using UCLUST (Edgar, 2010). Based on the sample with the minimum numbers of reads (Weiss et al., 2017), the sequences were clustered into 9,283 OTUs after excluding singletons and rarefying to 20,045 sequences per sample. The taxonomic identity of the bacterial OTU was then determined based on comparisons against the Silva database (https://www.arb-silva.de/). The OTUs for observed species number and Shannon indices were calculated in QIIME to evaluate microbial alpha diversity within samples.

2.6. Data analysis

The dissipations of CAP, Z1, and Z2 in the soil were described by first order kinetics:

- $C_t = C_0 e^{-kt}$,

where *t* represents the time (d) after the compounds application, C_0 represents the initial concentration of the compounds, C_t represents the concentrations at the time of *t*, and *k* is the rate constant (d^{-1}). The value of half-life (DT_{50}) was calculated as ln2/*k*.

The values in the tables and figures represent the means from the four replicates. Statistic data analysis was carried out by SPSS 19.0 (SPSS Inc., Chicago, IL, USA) and significance ($p < 0.05$) was determined using one way analysis of variance (ANOVA) via Tukey HSD comparison. Principal coordinates analysis (PCoA) based on Bray-Curtis distances was performed to examine the variation of bacterial community composition over the incubation period. The PCoA analysis was conducted in R (3.2.3) using the vegan package. The co-occurrence networks of the four treatments were created to visualize the interactions among different bacterial taxa using CoNet in CYTOSCAPE 3.7.1 (Faust et al., 2012). The OTUs were filtered by setting 8 (OTU) as the minimum occurrence across 16 samples within each treatment. The correlation was calculated using Pearson's correlation with a threshold of 0.8. Furthermore, to compute nodes and edges' attributes for each sample, the sub-networks were generated by preserving the presented nodes and edges from each sample as appeared in the network of each treatment. Then, Gephi (Bastian and Heymann, 2009) was used to visualize the co-occurrence networks of the four treatments and to calculate the topological characteristics of the sub-networks. The topological properties of the sub-networks were calculated including the numbers of nodes and edges, ratio of the positive to negative interactions (P/N), the module number, and the average clustering coefficient (ACC).

3. Results and discussion

3.1. Spectroscopic data and structural identification of CAP transformation byproducts

Using a preparative chromatograph, we successfully isolated two potential CAP transformation byproducts, Z1 and Z2. The characterization of their chemical structures was performed using spectroscopic techniques, including ^{1}H NMR, ^{13}C NMR, ^{1}H-^{13}C HSQC, and HRMS (Fig. S2-S10). The detailed spectroscopic data as well as the melting points (mp.) of both Z1 and Z2 are shown below.

Compound Z1: mp. 200 °C. ^{1}H NMR (400 MHz, $CDCl_3$) δ 10.21 (s, 1H), 8.38 (s, 1H), 7.77 (d, *J* = 7.3 Hz, 1H), 7.30 (s, 1H), 7.19 (s, 1H), 7.12 (d, *J* = 7.1 Hz, 1H), 7.06 (d, *J* = 7.1 Hz, 1H), 7.01 (s, 1H), 6.17 (s, 1H), 2.84 (s, 3H), 2.13 (s, 3H). ^{13}C NMR (101 MHz, $CDCl_3$) δ 169.54, 155.87, 149.11, 146.84, 139.28, 138.90, 136.43, 133.74, 133.58, 129.74, 129.11, 128.25, 126.40, 125.68, 124.32, 110.72, 26.80, 19.08. HRMS (ESI): calcd. for $C_{18}H_{15}BrClN_5O_2$ $[M + H]^+$ 448.0176; found 448.0178.

Compound Z2: mp. 191.5-193.0 °C. ^{1}H NMR (400 MHz, $CDCl_3$) δ 10.10 (s, 1H), 8.42 (d, *J* = 1.9 Hz, 1H), 7.93 (d, *J* = 1.9 Hz, 1H), 7.15 (s, 1H), 7.12 (s, 1H), 7.10 (s, 1H), 6.12 (d, *J* = 4.8 Hz, 1H), 2.87 (d, *J* = 4.9 Hz, 3H), 2.09 (s, 3H). ^{13}C NMR (101 MHz, $CDCl_3$) δ 168.43, 156.16, 147.95, 147.84, 141.00, 138.87, 138.56, 133.05, 132.21, 132.07, 131.71, 129.65, 128.63, 124.36, 121.38, 111.14, 26.92, 18.85. HRMS (ESI): calcd. for $C_{18}H_{13}Br_2Cl_2N_5O_2$ $[M + H]^+$ 561.8871; found 561.8828.

The CAP ^{1}H NMR and ^{13}C NMR findings have been previously reported (Lahm et al, 2007; Xu et al., 2009). By comparing the ^{13}C NMR spectrograms of Z1, Z2, and CAP, we see that they have the same number of carbon molecules and very similar

chemical shifts at the ^{13}C NMR spectrograms. The ^{1}H NMR spectrograms also showed that most of the hydrogen atoms in the three compounds followed very similar chemical shifts. That indicates that all three compounds have the same structural molecular skeleton. The difference among the NMR spectrograms between the three compounds is that Z1 had one more pyridyl-hydrogen ring and Z2 had one less as compared to CAP in the ^{1}H NMR. This was also confirmed by the ^{1}H-^{13}C HSQC Z1 and Z2 spectrograms, which showed that there were 7 and 5 aromatic C-H direct correlations respectively. We deduced that the chlorine atom was removed from the pyridine heterocyclic ring of CAP (Z1, Fig. 1) and was transformed to the following molecule $C_{18}H_{15}BrClN_5O_2$, which was further confirmed by the high-resolution mass spectra (HRMS, $[M + H]^+$=448.0176). For Z2; as the ortho coupling of hydrogen disappeared on the pyridine heterocyclic ring, we deduced that the meta-hydrogen of the chlorine atom was substituted. The most likely replacement for hydrogen in this system is Cl or Br. Through the HRMS result, we could confirm that the Br replaced the meta-hydrogen and gave the molecular formula of $C_{18}H_{13}Br_2Cl_2N_5O_2$ (Z2, Fig. 1). The chemical structure of Z2 was also confirmed by comparing the ^{1}H NMR spectrogram of Z2 with the literature (He et al., 2018).[25] After the structure identification, Z1 and Z2 were confirmed as the byproducts of CAP.

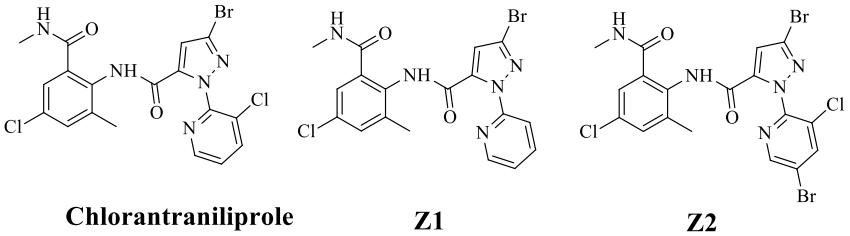

Fig. 1. Chemical structures of Chlorantraniliprole and its transformation byproducts Z1 and Z2

Due to the low concentration of the pesticide in soil, it was very difficult to isolate all possible transformation byproducts. In this study, from the dissipation process of the CAP in soil we found two relatively stable byproducts. When the soil was subjected to higher CAP dose, adequate Z1 and Z2 could be isolated after a month's incubation for further chemical structure identification. The compound Z2 has been previously reported as a synthetic derivative of CAP (He et al., 2018), while Z1 is a completely new compound without any recorded chemical structure data available. Here, we confirmed the presence of a new compound, Z1, as a CAP transformation byproduct and provide with its spectroscopic data. Previous studies mainly focused on the hydrolysis (Sharm et al., 2014) and photolysis products (Gaddamidi et al., 2011; Lavtizar et al., 2014) of CAP. Most of the reported transformation byproducts had different carbon skeletons compared to their parent compound (CAP); however, our study showed that the main transformation products identified in soil had same carbon skeleton with CAP. The pesticide dissipation process in soil is significantly affected by soil microbes, microbially-mediated dissipation process may differ from hydrolysis and photolysis. Sinclair and Boxall (2003) found that over 90% of the observed toxicity of the byproducts could be explained by the persistence of a toxicophore of the parent compound as well as from the differences in chemical uptake or the way the agent acts. On one hand, Z1 and Z2 have the same carbon skeleton as CAP; thus, byproucts maintained the toxic nucleus of CAP. On the other hand, they have different substitutes on the pyridine heterocyclic ring; thus, they may have different dissipation rates and toxicity levels. Therefore, the toxicites of both Z1 and Z2 require further attention.

3.2. Dissipation kinetics of CAP and its transformation byproducts

After 78 days of incubation, approximately 61.4% of CAP, 78.1% of Z1, and 73.5% of Z2 dissipated in soil (Fig. 2). Their dissipation kinetics followed first order reaction kinetics (r^2 > 0.96) with half-lives of 57.8, 38.5 and 43.3 d for CAP, Z1, and Z2, respectively (Fig. 2). Our results indicate that the dissipation of CAP in the soil is very slow, just like United States Environmental Protcction Agency (USEPA) has mentioned, CAP is characterized as a persistent pesticide in the terrestrial environment (USEPA, 2008). We found that the dissipation rates of both Z1 and Z2 were faster than that of CAP, which means that Z1 and Z2 were difficult to accumulate in soil, and this also explains the low concentrations of the CAP byproducts in soil.

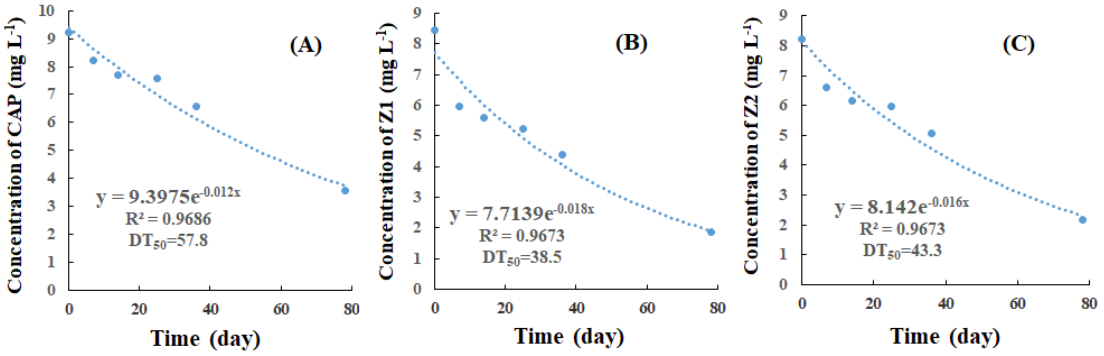

Fig. 2. Dissipation kinetics of CAP (A), Z1 (B), and Z2 (C) in soil. The best fit curves together with the kinetic equations and half-lives (DT_{50}) are included. Data are means of four replicates.

3.3. Risk evaluation of CAP and its byproducts on soil bacterial community

Soil bacteria account for the largest proportion of soil microorganisms and is very sensitive to external factors. The changes of the bacterial community was chosen as an indicator to evaluate the ecological impact and/or risk of CAP and its transformation byproducts to soil. Our previous work has shown that the bacterial community composition in soil was significantly affected by CAP application (1 mg kg^{-1} a.i./dw –

switched at day 14, and recovered at day 36) (Wu et al., 2018). Thus, the ecological risk of the three compounds was evaluated using the same timeframe as reference - 36 days of dissipation process.

3.3.1. Diversity and composition of the bacterial community

The alpha diversities of the bacterial communities during the dissipation process are shown in Fig. 3. The number of classifiable OTUs was significantly higher in CK ($p < 0.05$) than that from other treatments (CAP, Z1, and Z2) during the first 36 days. This demonstrates the potential toxicity of CAP and its byproducts towards the soil bacterial community. Z2 also had a significantly lower Shannon index than CK from day 14 to 36 ($p < 0.05$), which indicates that Z2 had a bigger impact to the bacterial diversity than CAP and Z1.

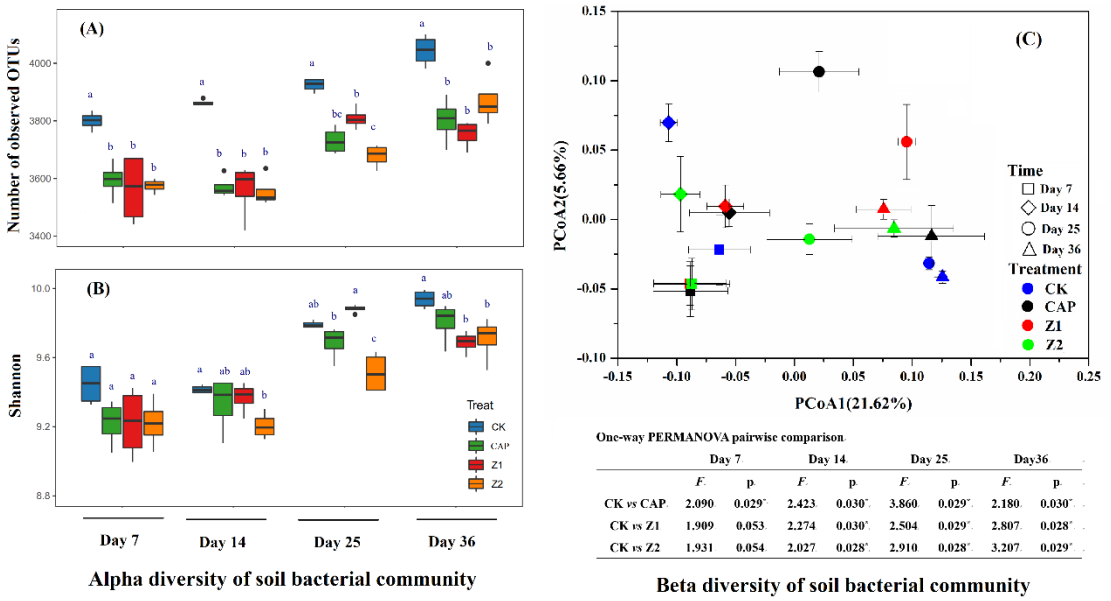

Fig. 3. Alpha and beta diversity of the soil bacterial community during pesticides dissipation process. The number of observed OTUs (**A**) and Shannon (**B**) index were used to characterize the alpha diversity. The significant differences in alpha diversity among different treatments at each sampling time was tested by one-way ANOVA ($p < 0.05$) and labeled with different lowercase letters. Beta

diversity was analyzed by principal co-ordinates analysis (PCoA) based on Bray-Curtis distance and displayed in scatter diagram (**C**). One-way PERMANOVA pairwise comparison was applied to compare the community variation of different treatments at each sampling time, the asterisk stands for statistically significant difference ($p < 0.05$).

The diagram Fig. 3C showed that the beta diversity was strongly affected by sampling time and compound types. Two-way PERMANOVA analysis confirmed this observation also indicated that sampling time ($F = 7.334$, $p < 0.0001$) affected the community variation more than compound types ($F = 1.868$, $p < 0.001$). One-way PERMANOVA pairwise comparison was further used to compare the community variation between CK and other treatments (CAP, Z1, and Z2) at each sampling time. At day 7, only CAP significantly affected the community composition as compared to CK ($p < 0.05$). From day 7 to day 36, CAP, Z1, and Z2 all significantly affected the community composition ($p < 0.05$), with CAP having the greatest impact on the community composition as compared to Z1 and Z2 during the first 25 days, while Z1 and Z2 affected the beta diversity more than CAP between days 25-36 (according to the *F* values (Fig, 3C)). CAP had the greatest impact on community composition at day 25 ($F = 3.860$) and the effect became less apparent by day 36 ($F = 2.180$). On the contrary, the effect of Z1 and Z2 on beta diversity gradually increased with time. This shows that the impact of Z1 and Z2 to the bacterial community occurs at a slow pace, however, is more persistent in terms of how it influences the bacterial community composition as compared to CAP. In other words, CAP induced a greater community variation during the early stages of dissipation, while Z1 and Z2 had a greater impact

on the community composition after a longer dissipation period; especially Z2 that showed much higher *F* value than CAP at day 36.

At phylum level, CAP and its transformation byproducts significantly affected key phyla at different stages (Fig. S11). For example, CAP significantly increased the abundance of *Actinobacteria*, *Gemmatimonadetes* but decreased the abundance of *Bacteroidetes* as compared with CK at day 25 ($p < 0.05$). Z2 significantly increased the abundance of *Bacteroidetes and Proteobacteria* at day 14 and 25, respectively. In the meantime, Z2 also significantly decreased the abundance of *Actinobacteria* and *Bacteroidetes* at day 7 and 36, respectively ($p < 0.05$). While Z1 showed no significant difference with CK at phylum level. These results indicate that the three compounds impose different effects on the soil bacterial community with Z2 likely having the greatest impact on the soil bacterial community compared to CAP and Z1.

3.3.2. Bacterial co-occurrence networks of CAP and its transformation byproducts

The co-occurrence networks (Fig. 4A-4D) of the soil bacterial communities under each treatment were analyzed based on strong and significant correlations. Overall, the bacterial co-occurrence networks were substantially different in structure, especially the Z2 networks that were more complicated than the other three ones formed (CK, CAP, and Z1). To statistically compare the network properties among individual treatments, 64 subnetworks (4 treatments ×16 replicates) were generated based on each sample (type and sampling time). The topological properties of the subnetworks that are typically used in network analysis were calculated to describe the complex relationships between soil bacterial communities (Table 1).

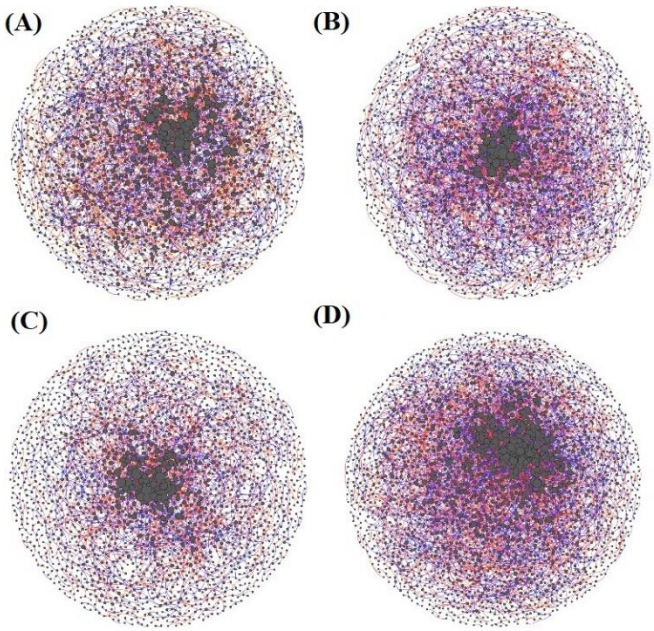

Fig. 4. The co-occurrence networks of soil bacterial communities under different treatments. A connection stands for a strong (correlation threshold $p > 0.8$) and significant ($p < 0.05$) correlation for the CK (A), CAP (B), Z1 (C), and Z2 (D) networks. The size of each node is proportional to the connection degrees. The red edges indicate the positive interactions between nodes, while the blue edges indicate the negative interactions.

Table 1 Topological features of co-occurrence networks of different treatments

Index	CK	CAP	Z1	Z2
Number of nodes	1695 b	1623 c	1664 b	1898 a
Number of edges	1515 c	1467 c	1629 b	2788 a
P/N	1.39 a	1.19 b	1.33 a	1.20 b
Module Number	3.48 b	5.89 a	3.72 b	5.99 a
ACC	0.20 a	0.16 c	0.17 b	0.19 a

Notes: P/N, ratio of positive to negative interactions; ACC, average clustering coefficients. The data

368 are the means of 16 replicates. Different letters indicate the significant differences among different
369 treatments by Turkey HSD tests ($p < 0.05$).

370 Specifically, the network of the control samples (CK) consisted of 1695 nodes (e.g.,
371 taxa) and 1515 edges (associations between taxa), while the CAP network showed less
372 nodes, Z1 showed more edges than CK. The Z2 network consisted of 1898 nodes and
373 2788 edges, which were significantly higher than the networks from all other three
374 treatments. This indicates that the network connectivity and complexity were highest
375 in Z2 treatment. Generally, the topological properties of Z1 networks were similar to
376 CK indicating that Z1 had a relatively little impact on the bacterial co-occurrence
377 network. Both CAP and Z2 showed significantly lower P/N and higher module numbers
378 than CK, which indicates that CAP and Z2 enhances the competitions of taxa and
379 increases the modularity in co-occurrence patterns. Higher modularity usually indicates
380 greater ecological stability of networks and reveals the potential of the community to
381 resist towards exogenous environmental factors (Krause et al., 2003). The taxa with
382 positive links in the networks are expected to easily co-oscillate while those with
383 negative links are considered more stable against co-oscillation (Coyte et al., 2015),
384 thus, the lower P/N also indicates the greater ecological stability of the networks (de
385 Vries et al., 2018). The results demonstrate that CAP and Z2 significantly affect the
386 bacterial co-occurrence network to make it more resistant to further environmental
387 stresses. Previous work showed that the pathogens that infect plants exhibit more
388 complex and highly connected bacterial networks compared to the network from
389 microbiota habiting healthy plants (Hu et al., 2020). It is generally considered that

invasive pathogenic microbes could generate positive feedback which enhances the competitiveness among the bacterial taxa in the network, and as such, the soil community structure is shaped. Similarly, in this study, CAP and Z2 forced the bacterial taxa to increase competitiveness, and subsequently promote network stability, to respond against the environmental perturbations.

3.3.3. Comprehensive risk assessment and implications of CAP and its byproducts

The three compounds CAP, Z1, and Z2 all decreased the bacterial OTU richness and changed the bacterial community composition. This indicates that all three compounds account as a potential ecological risk for the soil. The Z1 bacterial co-occurrence network had similar topological properties with that of CK, and also showed no significant difference with latter at phylum level. Therefore, Z1 was the least harmful to the soil bacterial community. Thus, the ecological risk of Z1 is minimal during the CAP dissipation process considering the rapid dissipation rate of the former (compared to CAP and Z2) as well as the low concentration of the CAP in the soil. Z2 had the strongest impact on both alpha (Shannon index) and beta diversities of the soil bacterial community during the dissipation process. Z2 also had the biggest impact on the soil taxa composition, at phylum level, compared to CAP and Z1. On the other hand, the bacterial co-occurrence network of Z2 was the most complicated and well-connected, and was also defined as more competitive than that of CK. This means that more taxa were selectively enriched while others excluded in the Z2 network. This indicates that the response of the taxa subjected to Z2 varies and subsequently the affinity of cells for this chemical is not consistent or similar to that of CAP. Thus, Z2 has a higher potential

412 ecological risk than its parent compound CAP.

413 In real situations, CAP, Z1 and Z2 could coexist in a certain period of time when
414 CAP is applied. As Z1 and Z2 dissipate faster than CAP, when the latter is applied at
415 low concentration (1 mg kg^{-1} a.i./dw) in soil, Z1 and Z2 are difficult to accumulate and
416 their ecological risks can practically remain under control. Generally, if CAP is applied
417 following the field recommended dosage, the ecological risk from the transformation
418 products could be negligible and only the risk from CAP itself should be considered.
419 However, when CAP is improperly applied at higher concentrations (≥10 mg kg^{-1}
420 a.i./dw) in some very special circumstances, Z2 is expected to build up and appear in
421 detectable concentrations in soil. In this circumstance, the ecological risks of Z2 would
422 deserve special attention and mitigation strategies would have to be considered and
423 executed. Besides, soil type and other conditions such as temperature, moisture in real
424 fields could also affect the affect the metabolism and transformation of CAP. For
425 example, it was found that the degradation rates of CAP and its impact on the microbial
426 community composition were different in the three paddy soils with different parent
427 materials (Wu et al., 2017). Thus, the type and concentration of CAP transformation products
428 may vary in different soil conditions. Regardless, this study highlights the concern and
429 the potential risk from the pesticides dissipation process byproducts that may emerge
430 and impact the quality of soil ecosystem, especially when applied at uncontrolled doses.

431 **4. Conclusions**

432 In this study, two transformation byproducts (Z1, Z2) from the pesticide
433 Chlorantraniliprole (CAP) dissipation process in soil were extracted and identified.

Assessment of the dissipation kinetics of the three chemicals showed that the two byproducts (Z1, Z2) had faster dissipation rates than that of CAP. The ecological risk assessment of CAP, Z1, and Z2 on soil was evaluated by assessing the influence of the three chemicals on the bacterial community habiting in it. The results showed that all the three can become a potential ecological risk as they all decrease the bacterial OTU richness and change the community composition as well as the interactive relationships between taxa within the bacterial community. However, the extent of the risk from these 3 compounds varies as per their influence on the alpha and beta diversities of the soil bacterial community and the topological features of the bacterial co-occurrence networks for each one. When the three compounds applied at same dose, the byproduct Z2 has the biggest potential impact on the soil bacterial community and accounts as a potentially high ecological risk. These findings underline that the ecological risks from the transformation byproducts of a compound/pesticide need to be assessed so we can understand the potential risks when this compound is applied in the soil.

Acknowledgments

This work was financially supported by the National Natural Science Foundation of China (No. 42077021 and 41401258), and Natural Science Foundation of Jiangsu Province (BK20181510).

Appendix A. Supporting information

Supplementary data associated with this article can be found in the online version at…

Reference

Anastassiades, M.; Lehotay, S. J.; Stajnbaher, D.; Schenck, F. J. Fast and easy multiresidue method employing acetonitrile extraction/partitioning and "dispersive solid phase extraction" for the determination of pesticides residues in produce. *J. AOAC Int.* **2003**, *86*, 412–431. https://doi.org/10.1093/jaoac/86.2.412.

Bastian, M.; Heymann, S. Gephi: an open source software for exploring and manipulating networks, Proceedings of the Third International ICWSM Conference, **2009**, 361–362.

Boxall, A. B. A.; Sinclair, C. J.; Fenner, K.; Kolpin, D.; Maund, S. J. When synthetic chemicals degrade in the environment. *Environ. Sci. Technol.* **2004**, *38*, 368–375. https://doi.org/10.1021/es040624v.

Caporaso, J. G.; Kuczynski, J.; Stombaugh, J.; Bittinger, K.; Bushman, F. D.; Costello, E. K.; Fierer, N.; Pena, A. G.; Goodrich, J. K.; Gordon, J. I. QIIME allows analysis of highthroughput community sequencing data. *Nat. Methods* **2010**, *7*, 335–336. https://doi.org/10.1038/nmeth.f.303.

Cordova, D.; Benner, E. A.; Sacher, M. D.; Rauh, J. J.; Sopa, J. S.; Lahm, G. P.; Selby, T. P.; Stevenson, T. M.; Flexner, L.; Gutteridge, S.; Rhoades, D. F.; Wu, L.; Smith, R. M.; Tao, Y. Anthranilic diamides: a new class of insecticides with a novel mode of action, ryanodine receptor activation. *Pestic. Biochem. Physio.* **2006**, *84*, 196–214. https://doi.org/10.1016/j.pestbp.2005.07.005.

Coyte, K. Z.; Schluter, J.; Foster, K. R. The ecology of the microbiome: networks, competition, and stability. *Science* **2015**, *350*, 663–666. https://doi.org/10.1126/science.aad2602.

Edgar, R. C.; Haas, B. J.; Clemente, J. C.; Quince, C.; Knight, R. UCHIME improves sensitivity

and speed of chimera detection. *Bioinformatics* **2011**, *27*, 2194–2200. https://doi.org/10.1093/bioinformatics/btq461.

Edgar R. C. Search and clustering orders of magnitude faster than BLAST. *Bioinformatics* **2010**, *26*, 2460–2461. https://doi.org/10.1093/bioinformatics/btr381.

Faust, K.; Sathirapongsasuti, J. F.; Izard, J.; Segata, N.; Gevers, D.; Raes, J.; Huttenhower, C. Microbial co-occurrence relationships in the human microbiome. *PLoS Comput. Biol.* **2012**, *8*, e1002606–1002617. https://doi.org/10.1371/journal.pcbi.1002606.

Felicio, A. A.; Freitas, J. S.; Scarin, J. B.; Ondei, L. D.; Teresa, F. B.; Schlenk, D.; de Almeida, E. A. Isolated and mixed effects of diuron and its metabolites on biotransformation enzymes and oxidative stress response of Nile tilapia (Oreochromis niloticus). *Ecotox. Environ. Safe* **2018**, *149*, 248–256. https://doi.org/10.1016/j.ecoenv.2017.12.009.

Gaddamidi, V.; Zimmerman, W. T.; Ponte, M.; Ruzo L. Pyrolysis of [^{14}C]-Chlorantraniliprole in Tobacco. *J. Agric. Food Chem.* **2011**, *59*, 9424–9432. https://doi.org/10.1021/jf201995b.

Girones, L.; Oliva, A. L.; Marcovecchio, J. E.; Arias, A. H. Spatial Distribution and Ecological Risk Assessment of Residual Organochlorine Pesticides (OCPs) in South American Marine Environments. *Curr. Environ. Health Rep.* **2020**, *7*, 147–160. https://doi.org/10.1007/s40572-020-00272-7.

He, B.; Yao, Z. W.; Li, D. H.; Zuo, X.; Cheng, K. Preparation method of chlorantraniliprole impurity by simultaneous oxidation and bromination. Faming Zhuanli Shenqing **2018**, CN 108033944 A 20180515

Hu, Q. L.; Tan, L.; Gu, S. S.; Xiao, Y. S.; Xiong, X. Y.; Zeng, W.; Feng, K.; Wei, Z.; Deng Y. Network analysis infers the wilt pathogen invasion associated with non-detrimental bacteria. *npj*

Biofilms Microbi. **2020**, *6*, 8. https://doi.org/10.1038/s41522-020-0117-2.

Krause, A. E.; Frank, K. A.; Mason, D. M.; Ulanowicz, R. E.; Taylor, W. W. Compartments revealed in food-web structure. *Nature* **2003**, *426*, 282–285. https://doi.org/10.1038/nature02115.

Lahm, G. P.; Selby, T. P.; Freudenberger, J. H. Insectedal anthranilic diamides: a new class of potent ryanodine receptor activators. *Bioorg. Med. Chem. Lett.* **2005,** *15*, 4898–4906. https://doi.org/10.1016/j.bmcl.2005.08.034.

Lahm, G. P.; Stevenson, T. M.; Selby, T. P.; Freudenberger, J. H.; Cordova, D.; Flexner, L.; Bellin, C. A.; Dubas, C. M.; Smith, B. K.; Hughes, K. A.; Hollingshaus, J. G.; Clark, C. E.; Benner, E. A. Rynaxypyr (TM): A new insecticidal anthranilic diamide that acts as a potent and selective ryanodine receptor activator. *Bioorg. Med. Chem. Lett.* **2007**, *17*, 6274–6279. https://doi.org/10.1016/j.bmcl.2007.09.012.

Lavtizar, V.; van Gestel, C. A. M.; Dolenc, D.; Trebše P. Chemical and photochemical degradation of chlorantraniliprole and characterization of its transformation products. *Chemosphere* **2014**, *95*, 408–414. https://doi.org/10.1016/j.chemosphere.2013.09.057.

Pietrzak, D.; Kania, J.; Kmiecik, E.; Malina, G.; Wator, K. Fate of selected neonicotinoid insecticides in soil-water systems: Current state of the art and knowledge gaps. *Chemosphere* **2020**, *255*, 126981. https://doi.org/10.1016/j.chemosphere.2020.126981.

Pimentel, D.; Hepperly, P.; Hanson, J.; Douds, D.; Seidel, R. Environmental, energetic, and economic comparisons of organic and conventional farming systems. *Bioscience* **2005**, *55 (7)*, 573–582. https://doi.org/10.1641/0006-3568(2005)055[0573:EEAECO]2.0.CO;2.

Roberts, T. R.; Hutson, D. H. Metabolic Pathways of Agrochemicals: Part 2, Insecticides and Fungicides. The Royal Society of Chemistry, Cambridge, UK. **1999**.

522 Redman, Z. C.; Anastasio, C.; Tjeerdema, R. S. Quantum yield for the aqueous photochemical
523 degradation of chlorantraniliprole and simulation of its environmental fate in a model california
524 rice field. *Environ. Toxicol. Chem.* **2020**, *39*, 1929–1935. https://doi.org/10.1002/etc.4827.
525 Redman, Z. C.; Parikh, S. J.; Hengel, M. J.; Tjeerdema, R. S. Influence of flooding, salinization,
526 and soil properties on degradation of chlorantraniliprole in california rice field soils. *J. Agric.*
527 *Food Chem.* **2019**, *67*, 8130–8137. https://doi.org/10.1021/acs.jafc.9b02947.
528 Schloss, P. D.; Westcott, S. L.; Ryabin, T.; Hall, J. R.; Hartmann, M.; Hollister, E. B.; Lesniewski,
529 R. A.; Oakley, B. B.; Parks, D. H.; Robinson, C. J.; Sahl, J. W.; Stres, B.; Thallinger, G. G.;
530 Van Horn, D. J.; Weber, C. F. Introducing mothur: open-source, platform-independent,
531 community-supported software for describing and comparing microbial communities. *Appl.*
532 *Environ. Microb.* **2009**, 75, 7537−7541. https://doi.org/10.1128/AEM.01541-09.
533 Schwarz, T.; Snow, T. A.; Santee, C. J.; Mulligan, C. C.; Class, T.; Wadsley, M. P.; Nanita, S. C.
534 QuEChERS multiresidue method validation and mass spectrometric assessment for the novel
535 anthranilic diamide insecticides chlorantraniliprole and cyantraniliprole. *J. Agric. Food Chem.*
536 **2011**, *59*, 814−821. https://doi.org/10.1021/jf103468d.
537 Sharma, A. K.; Zimmerman, W. T.; Lowrie, C.; Chapleo, S. Hydrolysis of chlorantraniliprole and
538 cyantraniliprole in various ph buffer solutions. *J. Agric. Food Chem.* **2014**, *62*, 3531−3536.
539 https://doi.org/10.1021/jf500671w.
540 Sinclair, C. J.; Boxall, A. B. A. Assessing the ecotoxicity of pesticide transformation products.
541 *Environ. Sci. Techno.* **2003**, *37*, 4617–4625. https://doi.org/10.1021/es030038m.
542 Teixeira, L. A. F.; Gut, L. J.; Wise, J. C.; Isaacs, R. Lethal and sublethal effects of chlorantraniliprole
543 on three species of Rhagoletis fruit flies (Diptera: Tephritidae). *Pest Manag. Sci.* **2009**, *65*,

137–143. https://doi.org/10.1002/ps.1657.

USEPA. Pesticide Fact Sheet: Chlorantraniliprole. U.S. Environmental Protection Agency, Washington, DC. **2008**.

de Vries, F. T.; Griffiths, R. I.; Bailey, M.; Craig, H.; Girlanda, M.; Gweon, H. S.; Hallin, S.; Kaisermann, A.; Keith, A. M.; Kretzschmar, M. Soil bacterial networks are less stable under drought than fungal networks. *Nat. Commun.* **2018**, *9*, 3033. https://doi.org/10.1038/s41467-018-05516-7.

Weiss, S.; Xu, Z. Z.; Peddada, S.; Amir, A.; Bittinger, K.; Gonzalez, A.; Lozupone, C.; Zaneveld, J. R.; Vazquez-Baeza, Y.; Birmingham, A.; Hyde, E. R.; Knight, R. Normalization and microbial differential abundance strategies depend upon data characteristics. *Microbiome* **2017**, *5*, 27. https://doi.org/10.1186/s40168-017-0237-y.

Wu, M.; Li, G. L.; Chen, X. F.; Liu, J.; Liu, M.; Jiang, C. Y.; Li, Z. P. Rational dose of insecticide chlorantraniliprole displays a transient impact on the microbial metabolic functions and bacterial community in a silty-loam paddy soil. *Sci. Total Environ.* **2018**, *616*, 236−244. https://doi.org/10.1016/j.scitotenv.2018.11.012.

Wu, M.; Liu, J.; Li, W. T.; Liu, M.; Jiang, C. Y.; Li, Z. P. Temporal dynamics of the compositions and activities of soil microbial communities post-application of the insecticide chlorantraniliprole in paddy soils. *Ecotox. Environ. Safe.* **2017**, *144*, 409−415. https://doi.org/10.1016/j.ecoenv.2017.06.056.

Xu, J. Y.; Dong, W. L.; Xiong, L. X.; Li, Y. X.; Li, Z. M. Design, Synthesis and biological activities of novel amides (sulfonamides) containing n-pyridylpyrazole. *Chinese J. Chem.* **2009**, *27*, 2007−2012. https://doi.org/10.1002/cjoc.200990337.

566 Zhang, J. M.; Chai, W. G.; Wu, Y. L. Residues of chlorantraniliprole in rice field ecosystem.

567 *Chemosphere* **2012**, *87*, 132–136. https://doi.org/10.1016/j.chemosphere.2011.11.076.